Research Article

GAZİ
JOURNAL OF ENGINEERING SCIENCES

A Study on Four-Bar Mechanism with Constant Coupler Point Velocity: Modelling, Numerical Simulation and Experimental Application

Halit Hülako*[a], Orhan Çakar[b]

Submitted: 30.10.2024 Revised: 10.02.2024 Accepted: 14.10.2025 doi:10.30855/gmbd.070525N01

ABSTRACT

In industry, the trace path of a point on the coupler link of four-bar mechanism is often utilized and sometimes it is desired that the couplar point moves on its path with constant velocity. This can be achieved by a variable crank speed. Processes requiring constant speed are often achieved by designing expensive complex mechanisms with high degrees of freedom without feedback control. This study considers the four-bar mechanism driven by a DC motor with constant coupler point velocity. MATLAB® is used to model and to simulate the system dynamics. We have successfully implemented an experimental application of coupler point speed control, a mechanism that is much needed in the industry, at a remarkably low cost. We developed a highly detailed simulation model that incorporates intricate system dynamics including bearing frictions. Additionally, motor parameters are predicted for the application through cost-effective estimation techniques. In order to show the efficiency of the method, some experimental studies are made besides the numerical simulations and the results are compared. Proportional plus integral plus derivative (PID) control action is used to control of the crank speed and it is shown that the desired coupler point velocity is achieved.

Keywords: Coupler Point, Four-Bar Mechanism, Crank Speed Control, Simscape Multibody Model

[a*] Hakkari University,
Engineering Faculty,
Dept. of Mechanical Engineering
30000 - Hakkari, Türkiye
Orcid: 0000-0001-8194-5433
e mail: halithulako@hakkari.edu.tr

[b] Fırat University,
Engineering Faculty,
Dept. of Mechanical Engineering
23000 - Elazığ, Türkiye
Orcid: 0000-0001-6947-3875
e mail: cakaro@firat.edu.tr

*Corresponding author:
halithulako@hakkari.edu.tr

Dört Çubuk Mekanizmasında Bir Biyel Noktasında Sabit Hız Elde Etmeye Yönelik Bir Çalışma: Modellemesi, Sayısal Simülasyonu ve Deneysel Uygulaması

ÖZ

Endüstride, dört çubuklu bir mekanizmanın biyel kolundaki bir noktanın izlediği yol sıklıkla kullanılmakta ve bazen bu biyel noktasının yörüngesi üzerinde sabit hızla hareket etmesi istenmektedir. Bu, değişken krank hızı ile sağlanabilir. Sabit hız gerektiren süreçler, genellikle geri besleme kontrolü olmaksızın yüksek serbestlik derecesine sahip pahalı ve karmaşık mekanizmalar tasarlanarak gerçekleştirilir. Bu çalışma, biyel noktasının sabit hızını sağlamak üzere bir DC motoru tarafından tahrik edilen dört çubuklu bir mekanizmayı ele almaktadır. Sistem dinamiklerini modellemek ve simüle etmek için MATLAB® kullanılmıştır. Sanayinin büyük ölçüde ihtiyaç duyduğu biyel noktası hız kontrolünün deneysel bir uygulaması, dikkate değer derecede düşük bir maliyetle başarıyla gerçekleştirilmiştir. Detaylı bir simülasyon modeli geliştirilmiş ve bu model, yatak sürtünmeleri gibi karmaşık sistem dinamiklerini içermektedir. Ayrıca, uygulama için gerekli olan motor parametreleri, tahmin yöntemleriyle belirlenmiştir. Yöntemin etkinliğini göstermek için sayısal simülasyonların yanı sıra bazı deneysel çalışmalar yapılmış ve sonuçlar karşılaştırılmıştır. Krank hızını kontrol etmek için oransal, integral ve türev (PID) kontrol yöntemi kullanılmış ve istenilen biyel nokta hızının elde edildiği gösterilmiştir.

Anahtar Kelimeler: Biyel Noktası, Dört Çubuk Mekanizması, Krank Hız Kontrolü, Simscape Multibody Model

To cite this article: H. Hülako and O. Çakar, "A Study on Four-Bar Mechanism with Constant Coupler Point Velocity: Modelling, Numerical Simulation and Experimental Application", *Gazi Journal of Engineering Sciences,* vol.xx, no.x, pp. xx-xx, 2025. doi:10.30855/gmbd.070525N01

1. Introduction

Mass production machines generally have requirements such as high production speed, constant speed, product specific process trajectories and low cost. Four-bar mechanisms are widely used in industry and are classified as motion, function, or path generation based on requirements [1]. The mechanisms are designed assuming that the input link, i.e. crank, rotates at a constant speed. However, even if a constant voltage is supplied to the motor driving the crank of the four-bar mechanism, fluctuations occur around the desired speed of the crank due to the dynamics of the mechanism itself. To partially eliminate these speed fluctuations, a flywheel can be added to the crank mechanically. However, today, this is not sufficient, especially due to the need to use high-speed, light and flexible mechanisms. With the development of measurement tools and control engineering, these speed fluctuations can be eliminated more effectively by controlling the motor that drives the mechanism. For this purpose, the crank speed is measured instantaneously and compared with the reference value and the appropriate control signal is generated according to the present error and applied to the motor driving the mechanism to eliminate the speed fluctuation. Tao and Sadler [2] tried to eliminate the speed fluctuations occurring in the crank speed of a four-bar mechanism driven by a direct current (DC) electrical motor by implementing the well-known proportional plus integral plus derivative (PID) control action-based algorithms. Other control techniques, such as fuzzy logic [3], sliding mode control [4], moving sliding mode control [5], backstepping control [6], and a combination of these techniques [7,8], have also been used for the same purpose. Four-bar mechanisms that generate path are commonly used in the industry. These mechanisms typically utilize a point on the link, known as the coupler, and the path traced by this point is referred to as coupler curves. Fig. 1a shows the kinematic diagram of the four bar path generating mechanism and Fig. 1b shows the trajectory drawn by point C on the coupler link. The third link, or coupler, which connects the links 2 and 4 to each other, creates different curves based on the geometric position of the point C on it. When the input link is moves at a constant speed, the velocity of coupler point varies along the trajectory it follows, depending on the link lengths and the geometric position of C. In the industry, there are situations where it is desired that this point moves at a constant velocity in a specific portion or throughout the entire trajectory it follows. Designing mechanisms that can provide a constant speed in a specific region is possible [9,10]; however, due to the dynamics of the mechanism, this cannot be achieved accurately without control. While measuring the crank speed is easy in real applications, measuring the speed of a point moving along a trajectory is quite challenging and costly. In this regard, ensuring that the coupler point follows the trajectory at a constant speed can be achieved with a variable crank speed. This can be achieved by controlling the motor that drives the mechanism. For this purpose, a variable crank speed profile can be obtained from the kinematic relationship between the velocity of the coupler point and the crank speed. This velocity profile can be used as a reference to control the crank speed. Peón-Escalante et al. [11] tried to control the speed of the crank in a four-bar mechanism to ensure that a point on the coupler moves at a constant speed on the trajectory it follows. For this purpose, the dynamics of the four-bar mechanism driven by a DC motor were obtained analytically and the desired variable crank speed was tried to be achieved with the PID algorithm. Then Bañuelos et al. [12] presented their experimental studies on the same problem. In their work, they determined the velocity of the coupler point using real-time camera images and employed a PID control algorithm. Recently, Peón-Escalante et al. [13] applied Artificial Neural Network (ANN) based PID control scheme to the same problem. Denizhan and Chew explored linkage mechanisms for automotive applications, emphasizing the role of optimized spring configurations to reduce the force required to open and maintain hood positions. Their findings showed that extension and compression springs could effectively balance the hood while allowing ease of use [14]. The usual way of analysing mechanisms is to derive mathematical model of the system and solve them by numerical methods. However, especially for complex dynamic systems with high degrees of freedom, analyzing dynamics can be challenging. Another way to solve dynamic problems is through commercial simulation programs. MATLAB® provides a wide environment for such studies. With MATLAB® SIMULINK®, both the control structure and the dynamic model can be created and executed in the same environment using block structures. Multibody Simulation (MSM) formulates and solves the equation of motion after modeling the system with blocks such as forces, sensors, joints, and links [15]. This allows researchers to focus on their main studies without the need to derive the complex dynamic equations of the mechanism. For example, the complete dynamics of the robotic mechanism with 26 degrees of freedom were modelled by using MSM in [16]. The present study considers the problem of maintaining constant speed motion along the trajectory of a point on the coupler in a four-bar mechanism driven by a DC motor (see Fig. 1b). The MSM interface is used to model the dynamics of the system consisting DC motor-gearbox-four-bar linkage. However, the friction in the joints that has not been considered in other studies was taken into account. The crank speed was controlled using PID control technique with reference to the obtained variable crank speed profile for a specified coupler point velocity. In order to show the efficiency of the method, some

experimental case studies are made besides the numerical simulations. In the next section, the kinematic relationship between the velocity of the coupler point and the crank speed is determined. Then the system is modelled by using MSM tool and the numerical simulations and experimental case studies are given for the specific coupler point velocities with comparision. Subsequently, the results are discussed.

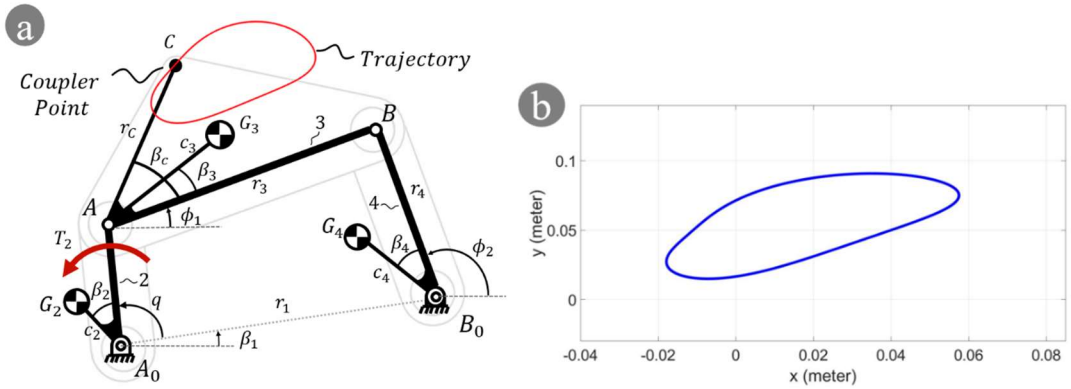

Fig. 1. (a) Kinematic diagram of the four-bar mechanism and (b) the tracking path of point C on the coupler link

2. Kinematic Modeling of System

In this section, the relationship between the coupler point velocity and the crank angular velocity is derived. The vector loop equation of the four-bar linkage mechanism given in Fig. 1a is:

$$\boldsymbol{A_0A} + \boldsymbol{AB} = \boldsymbol{A_0B_0} + \boldsymbol{B_0B} \tag{1}$$

and it can be written in the polar form as,

$$r_2 e^{iq} + r_3 e^{i\phi_1} = r_1 + r_4 e^{i\phi_2} \tag{2}$$

Two scaler equations can be written from Eq. (2) using Euler identity as follows:

$$f_1(q, \phi_1, \phi_2) = r_2 cosq + r_3 cos\phi_1 - r_1 - r_4 cos\phi_2 = 0 \tag{3}$$

$$f_2(q, \phi_1, \phi_2) = r_2 sinq + r_3 sin\phi_1 - r_4 sin\phi_2 = 0 \tag{4}$$

where ri, (i=1,2,3,4) represents length of links, q is position of input crank and ϕ_1, i=1,2 are positions of other links. For given q, ϕ_1 and ϕ_2 can be found by solving nonlinear equations given by Eq.(2) or Eqs.(3,4).

On the other hand, the angular velocities of links 2 and 3 $\dot{\phi}_1$ and $\dot{\phi}_2$ depending on the crank angular velocity $\dot{q}$ are given as follows:

$$\dot{\phi}_1 = g_1 \dot{q}, \quad \dot{\phi}_2 = g_2 \dot{q} \tag{5}$$

where g_1 and g_2 are named as velocity influence coefficients and they are calculated as follows:

$$\mathbf{g} = -\mathbf{J}^{-1}\mathbf{f}' \tag{6}$$

where the bold characters are vectors and matrices and **J** is Jacobian matrix, **g** is velocity influence coefficients vector and $\mathbf{f}'$ is the derivative of the constraint equations Eqs.(3,4) according to the input variable q and written in the form as:

$$\mathbf{g} = \{g_1\ g_2\}^T, \mathbf{f}' = \left\{\frac{\partial f_1}{\partial q} \quad \frac{\partial f_2}{\partial q}\right\}^T \tag{7}$$

$$J_{ij} = \frac{\partial f_i}{\partial \phi_j}, (i,j = 1,2) \tag{8}$$

For the four-bar linkage **J** ve $\mathbf{f}'$ are given as follows [5]:

$$\mathbf{J} = \begin{bmatrix} -r_3 sin\phi_1 & r_4 sin\phi_2 \\ r_3 cos\phi_1 & -r_4 cos\phi_2 \end{bmatrix}, \quad \mathbf{f}' = \begin{Bmatrix} -r_2 sinq \\ r_2 cosq \end{Bmatrix}, \tag{9}$$

Solving Eq.(6) the velocity influence coefficients of four-bar linkages can be found as follows:

$$g_1 = -\frac{r_2 \sin(q - \phi_2)}{r_3 \sin(\phi_1 - \phi_2)}, \tag{10}$$

$$g_2 = -\frac{r_2 \sin(q - \phi_1)}{r_4 \sin(\phi_1 - \phi_2)} \tag{11}$$

The next step is to express the angular velocity of the input crank $\dot{q}$ depending on the velocity of the coupler point V_C. The position vector of the coupler point can be written in the polar form as:

$$\boldsymbol{A_0C} = \boldsymbol{A_0A} + \boldsymbol{AC} \tag{12}$$

$$r_C = r_2 e^{iq} + r_C e^{i(\phi_1 + \beta_C)} \tag{13}$$

and the time derivative of Eq.(13) gives the coupler point velocity:

$$V_C = i r_2 \dot{q} e^{iq} + i r_C \dot{\phi}_1 e^{i(\phi_1 + \beta)} \tag{14}$$

and the real and imaginary parts are

$$V_C^x = -r_2 \dot{q} \text{sinq} - r_C \dot{q} g_1 \sin(\phi_1 + \beta_C) \tag{15}$$

$$V_C^y = r_2 \dot{q} \text{cosq} + r_C \dot{q} g_1 cos\ (\phi_1 + \beta_C) \tag{16}$$

Finally, the angular velocity of the input crank can be found as follows:

$$\dot{q} = \sqrt{\frac{(V_C^x)^2 + \left(V_C^y\right)^2}{r_2^2 + r_C^2 g_1^2 + 2 r_2 r_C g_1 \cos\,(q - \phi_1 - \beta_C)}} \tag{17}$$

The Eq.(17) gives the variable crank velocity for the given value of $V_C = \sqrt{(V_C^x)^2 + \left(V_C^y\right)^2}$ and it is reference for the control algorithm. Although the value of V_C is taken as constant during the trajectory in this study, it can be considered as partially constant or fully variable. It should be noted that, the necessary position and velocity values for the control will be determined by the mechanism model created in MSM environment, in this study. In the next section, the modelling of the linkage and control system in SIMULINK is given.

3. Modelling the System via MSM

The motion analysis is made in order to understand dynamic behaviour of a machine under the known external forces. This analysis is also called as forward dynamics or Wittenbauer's first problem. For this analysis, it is needed to derive equation of motion of the machine under consideration, first. There is a number of different ways to accomplish this, for example Exergian equation of motion for single degree of freedom

machines, and Lagrange Equations for single or multiple degree of freedom systems. On the other hand, today there are many commercial analysis programs and these offer researchers the opportunity to analyse without deriving the equation of motion. MATLAB® SIMULINK is a widely used tool where the system is simply modelled with blocks and connections. The mechatronic system under consideration in this study includes the four-bar linkage, DC motor-gearbox and the controller. The main block structure created in MSM is given in Fig.(2). The four-bar mechanism block has one input and four outputs. Input is DC motor torque and outputs are the position of links and the speed of crank. These outputs are the inputs of controller block. The controller block generates the control signal by comparing desired and present value of the crank speed. The DC motor block generates the control torque depending on the control signal and this torque drives the crank of mechanism from the torque input. In the next subsections, the detailed block structures of mechanism, DC motor with gearbox and controller are given.

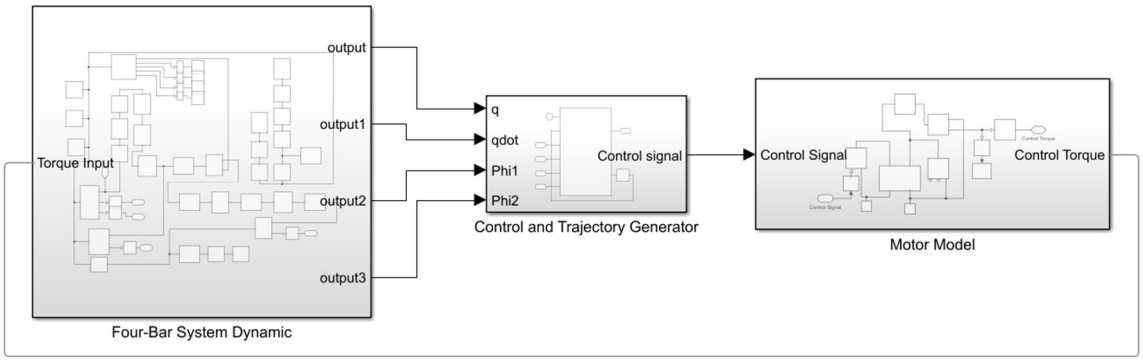

Fig. 2. Simulink® main model structure of a four-bar mechanism that follows a variable speed trajectory with DC motor control

3.1. Four-bar linkage model in MSM

The SIMULINK® block model of the four-bar linkage is shown in Fig.(3). Four-bar linkage consists of four rigid bodies (links) and four revolute joints. The rigid links can be created by using computer aided design (CAD) programs as well as using SIMULINK® library. The mass, mass moment of inertia, and mass centre of the linkage elements' physical parameters are automatically generated once the material parameters are defined. The revolute joints are defined between two links. The rigid transform blocks are used to define the position of the joints on the links taking the local coordinate of the relevant rigid link as reference. The damping and stiffness properties of joints can be defined in the joint blocks. However, the position and velocities of the links and the reaction forces in the joints during the motion can be determined from the joint blocks. For example, the outputs q and ω in the revolute joint 1-2 block are the angular position and the angular velocity of the link 2, respectively. In addition, the inner and outer ring bearing blocks are defined between the joint and the adjacent link compatible with the experimental case in this study. However, the frame of experimental system, DC motor body and couplings are transferred to SIMULINK model from CAD. It should be noted that Ports B and F are frame ports they represent the base and follower frames, respectively.

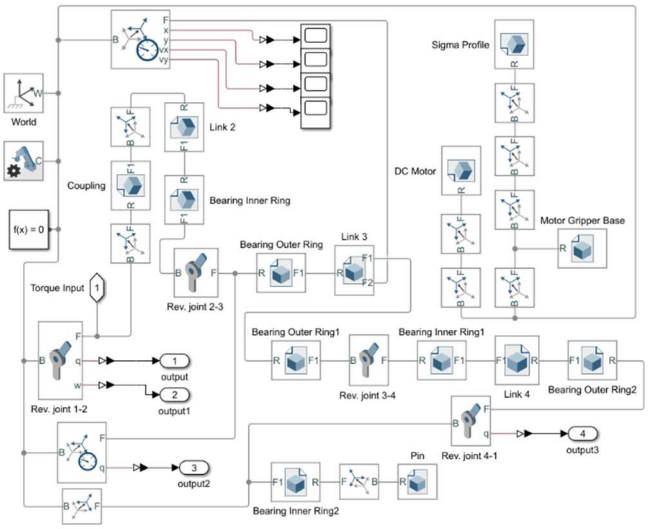

Fig. 3. Block diagram of the four-bar system dynamics subsystem

3.2. DC motor model in MSM

In this study it is considered that the mechanism is driven by a DC motor and a gear box as shown in Fig.(4). DC motor input voltage V_a, the torque generated by motor Tm and the torque at output of gearbox T2 are given by Eqs.(18-20), respectively [2-5].

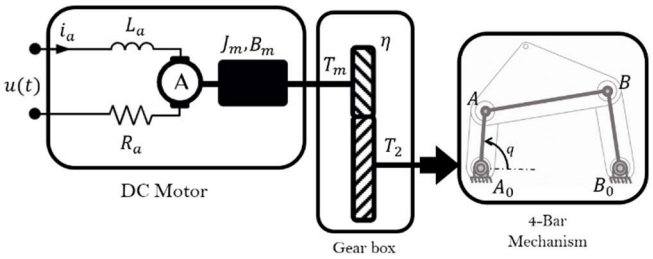

Fig. 4. DC motor-gearbox-four bar mechanism model

$$V_a = R_a i_a + L_a \frac{di_a}{dt} + nK_g \dot{q} \tag{18}$$

$$T_m = K_m i_a \tag{19}$$

$$T_2 = n(-nJ_m \ddot{q} - nB\dot{q} + T_m - T_f) \tag{20}$$

The definition of symbols used in Eqs.(18-20) are given as follows

Symbol	Unit	Description
Ra	Ω	Armature resistance
La	Henry	Armature inductance
ia	A	Armature current
Kg	V-s	Motor voltage constant
n	-	Gear ratio
Km	Nm/A	Motor torque constant
Tf	Nm	Lost torque due to friction in brushes, bearings, gearbox and so on.
Jm	kg-m2	Mass moment of inertia of the rotor
B	Nm-s	Viscous damping coefficient in the bearings

DC Motor model is ready in SIMULINK® as a block and it is shown in Fig.(5) including gearbox block. All of the motor parameters defined above are set in the DC motor block. Input of the block is the control voltage and the output is the control torque. The torque is measured by a torque sensor at output of gearbox block.

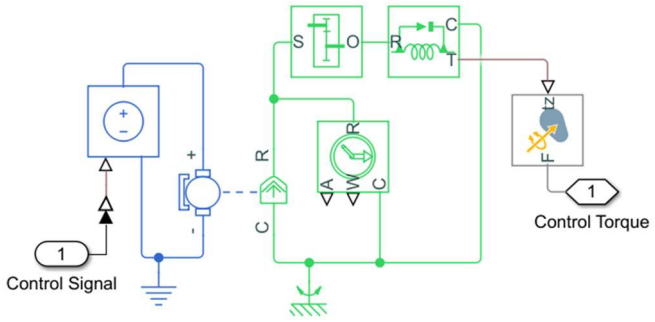

Fig. 5. DC Motor and gearbox block diagram

It should be stated that, MATLAB® Parameter Estimation toolbox can be used to estimate the actual DC motor parameters. The experimental performance outputs, such as the voltage and speed of the motor, are used to determine the motor parameters. DC motor parameters used in this study are determined MATLAB toolbox and then they are used in the simulations.

3.3. Speed trajectory generator and control

The control structure of the DC motor-four bar linkage is shown in Fig.(6). V_C^{des} is the desired velocity of the coupler point. The constant velocity of the coupler point is achieved with variable crank speed. The crank speed trajectory $\dot{q}_{trj}$ is generated by using Eq.(17) where the necessary position parameters (q, ϕ_1, ϕ_2) are taken from the four-bar linkage block. However, the instantaneous speed of the crank $\dot{q}$ is feed back to calculate speed error and the control signal $u(t)$ is generated by the controller. In this study PID controller is considered and the control signal is defined as

$$u(t) = K_p e(t) + K_d \frac{de(t)}{dt} + K_i \int_0^t e(t)\, dt \tag{21}$$

where K_p, K_d and K_i proportional, derivative and integral gains respectively, and $e(t)$ is the speed error defined as follows:

$$e(t) = \dot{q}_{trj} - \dot{q} \tag{22}$$

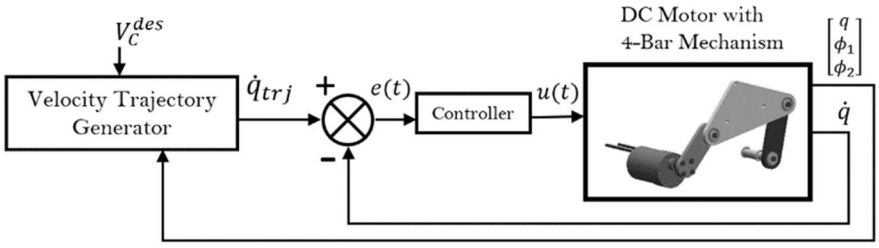

Fig. 6. The control structure of the DC motor-gearbox-four bar linkage

A MATLAB® function is prepared for the speed trajectory generator and the controller as a function block in MSM and given in Fig.(7).

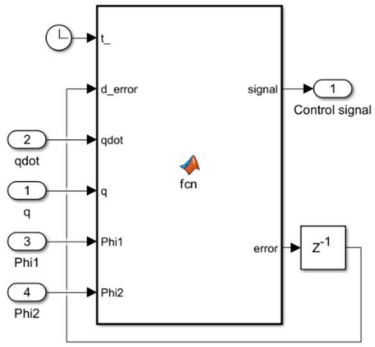

Fig. 7. The function block including trajectory generator and controller

In this way, the mechatronic system consists of DC motor-gearbox-fourbar linkage is modelled in MSM without deriving the complex equations of motions. In this study, some numerical simulations and experimental case studies have been made and the results are given in the followed two sections, respectively. In the applications, two diferent four-bar linkages named Model-1 and Model-2 are used. In the Model-2, the mass properties of the link 3 are changed in order to show the performance of the method. For the experimental studies, two four-bar mechanisms driven by a DC-Motor is manufactured and the same linkage and DC-motor parameters are used in both the numerical simulation and the experimental case studies.

4. Numerical Simulation

The parameters of Model-1 four-bar linkage and DC-motor used in the simulation are given in Table 1 and Table 2 respectively. 3D solid model of the four-bar linkage was created via SolidWorks and it is transferred to the Simscape as shown in Fig. 8. There is a gearbox with 1:50 gear ratio at the motor output. However, in the joints of the experimental system, the roller bearings with mass of 40 g are used and the mass of them are considered in the simulations. Also, the viscous friction in bearings is considered in the simulations. The viscous friction coefficient is determined by experimentally as 0.000745 $Nm/(rad/sec)$. For this, one of the link is subjected to the free vibration like a pendulum while other link is fixed and the damping coefficient is determined from logarithmic decrement.

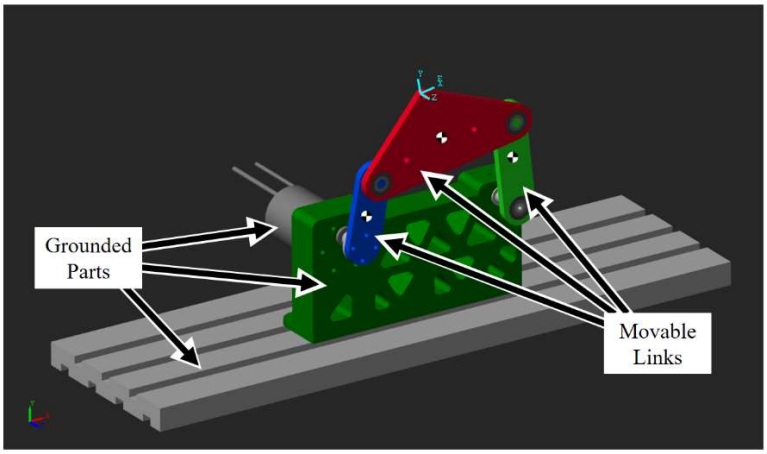

Fig. 8. 3D solid model of the four-bar linkage

Table 1. Four-bar linkage parameters

Mechanism parameters				
		Model 1-Link no (i)		
Parameters	1	2	3	4
r_i (mm)	108.91	42.26	96.44	58.78
c_i (mm)		21.13	0.04781	29.39
m_i (kg)		0.0461	0.1438	0.0546
J i (kg-m2)		1.55e-5	0.000125	2.91e-05
β i (rad)	0.0	0.0	0.2268	0.0
β c (rad)	r_c (mm)			
0.8318	58.11			

Table 2. DC motor parameters

DC Motor parameters						
R (Ω)	L (H)	K_m (Nm/A)	K_g (Vs)	J_m (kgm2)	T_f (Nm)	B (Nms)
4.2602	0.0538	0.0021	6.9724e-4	1.1236e-6	0.00	9.5486e-7
Power (kW)	Torque (Nm)	Speed (rpm) (Gearbox output)	Voltage (V)	Current (A)		
0.04	1.47	330	12	<6.0		

The simulations are made for the constant coupler point velocities $V_C^{des} = 0.1$ and $V_C^{des} = 0.2\ m/sec$. m/sec. PID parameters for Model 1 mechanism are determined by trial and error $K_p = 3.7, K_i = 7$ and $K_d = 2.$, as this approach allowed practical tuning for desired performance. However, methods like pole placement could also be considered for systematic tuning to ensure stability across various operating conditions. The simulations are run for 5 seconds using the chosen Ode4 (Runge-Kutta) solver with a fixed time step of 0.0001 seconds. The comparison of the desired and calculated (measured) angular velocity trajectories and the crank velocity errors for the cases $V_C^{des} = 0.1\ m/sec$ and $V_C^{des} = 0.2\ m/sec$ are given in Fig. 9 and Fig. 10, respectively. It is seen that the desired and measured crank velocities match each other well along the entire trajectory, and the error for both cases are under 0.1 rad/sec after 1.5 sec and they tend to decrease over time due to control.

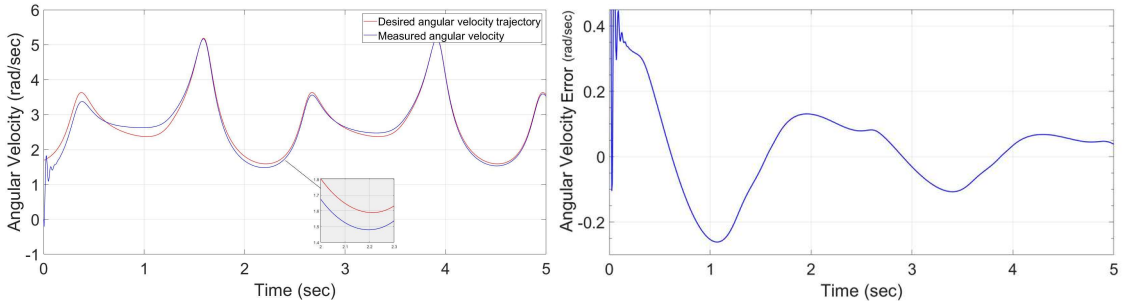

Fig. 9. a) Comparison of desired and calculated crank speeds and b) crank speed error of Model-1 mechanism for $V_C^{des} = 0.1\ m/sec$

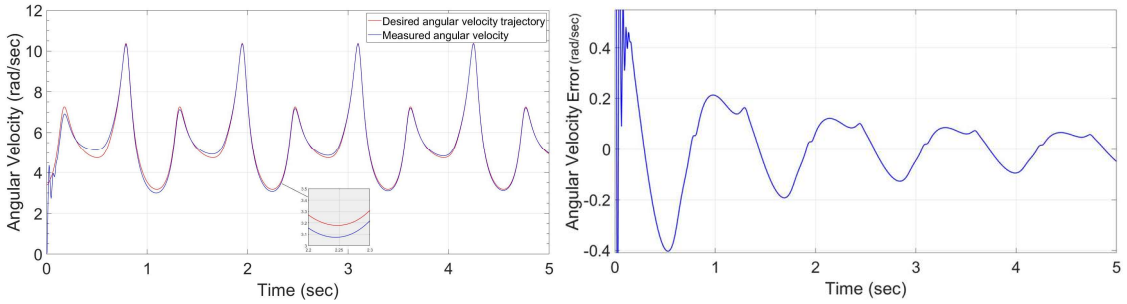

Fig. 10. a) Comparison of desired and calculated crank speeds and b) crank speed error of Model-1 mechanism for $V_C^{des} = 0.2\ m/sec$

In order to show the performance of the proposed method, a second simulation is conducted. In the second example, the mass and mass moment of inertia values of the link 3 are updated without changing the physical and geometrical properties of the other links such that $m_3 = 0.719$ kg and $J_3 = 0.000626$ kg·m^2. This model is named as Model-2. In this case, PID parameters are estimated as $K_p = 50$, $K_i = 30$ and $K_d = 10$. The results for this case are also very satisfactory as can be seen in Fig.s 11 and 12.

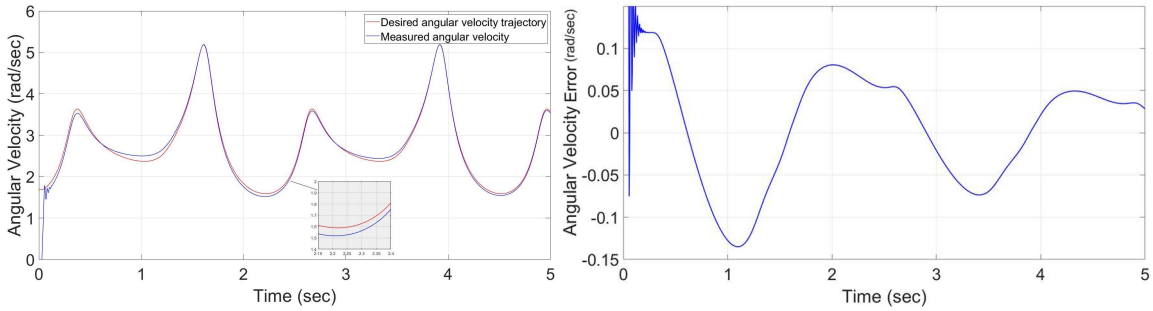

Fig. 11. a) Comparison of desired and calculated crank speeds and b) crank speed error of Model-2 mechanism fo $V_C^{des} = 0.1\ m/sec$

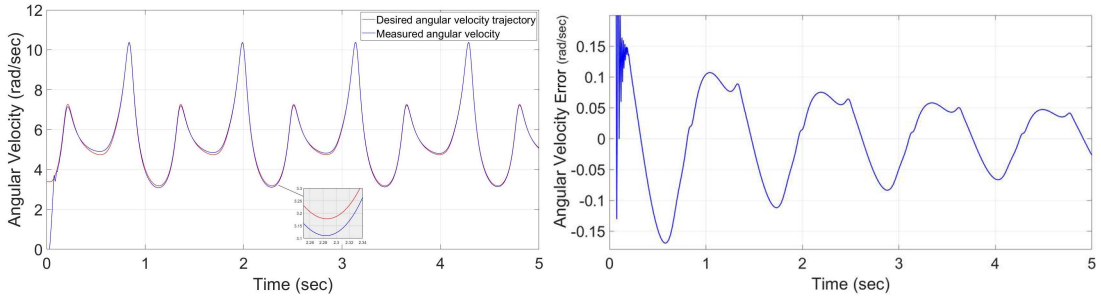

Fig. 12. a) Comparison of desired and calculated crank speeds and b) crank speed error of Model-2 mechanism for $V_C^{des} = 0.2\ m/sec$

5. Experimental Study

For the experimental study Model 1 and Model 2 mechanisms, are manufactured where moving parts links 2-4 are produced by laser cutting from steel sheet with thickness of 5 mm and fixed part link 1 is produced by 3D printing from PLA flament. For Model-2, the link 3 is manufactured thicker. A 12 V DC motor with a gear box and optical encoder, whose parameters are given in Table 2, is used to drive the crank. ATMEGA 328, 8 bit- 16 MHz microchip were used to control the system. The mechanism is controlled by the microcontroller at a frequency of approximately 200 Hz. The experimental system is shown in Fig. 13. It should be noted that 1 kHz PWM signal is generated for the motor driver and a low-pass filter on the encoder output was used to eliminate the noise.

For the experimental study, both Model-1 and Model-2 mechanisms are run for the cases constant coupler point velocities $V_C^{des} = 0.1$ and $V_C^{des} = 0.2\ m/sec$. PID control parameters are estimated using the trial-and-

error method as $K_p = 8,\ K_i = 12, K_d = 20$ for Model 1 and $K_p = 13,\ K_i = 50, K_d = 32$ for Model 2. The results for both mechanisms are given in Fig.s 14-17. As can be seen in the Fig.s, the measured crank speed agrees with desired crank speed trajectory but some noise. For these cases the trajectory errors are under 0.6 rad/sec.

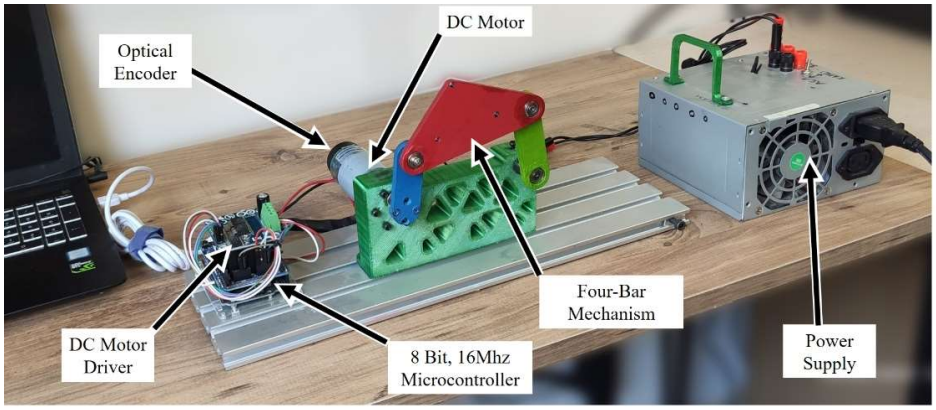

Fig. 13. Experimental system

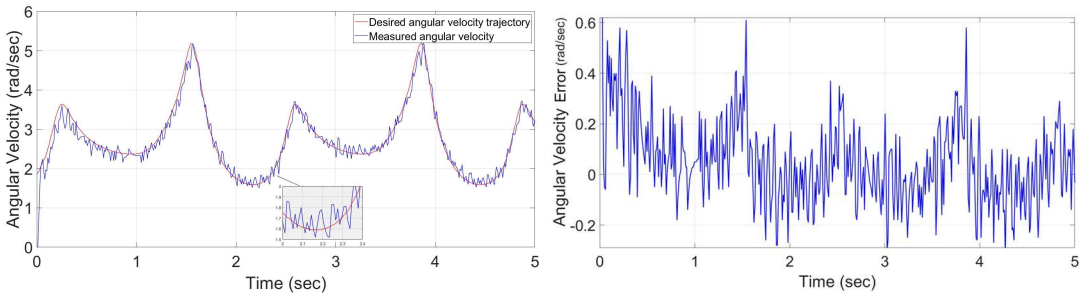

Fig. 14. a) Comparison of desired and measured crank speeds and b) crank speed error of Model-1 mechanism for $V_c^{des} = 0.1\ m/sec$

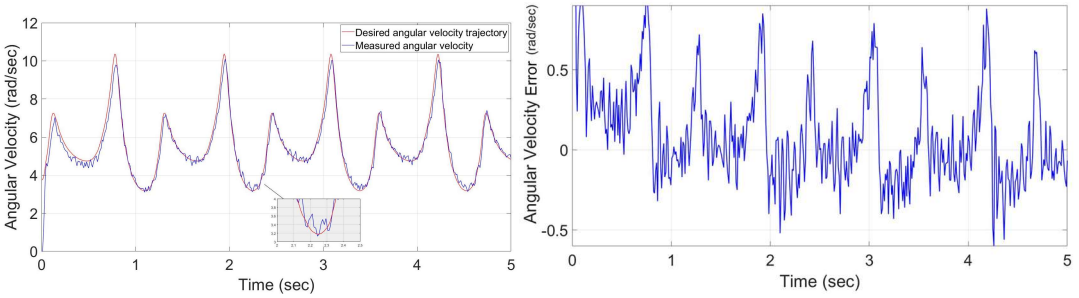

Fig. 15. a) Comparison of desired and measured crank speeds and b) crank speed error of Model-1 mechanism for $V_c^{des} = 0.2\ m/sec$

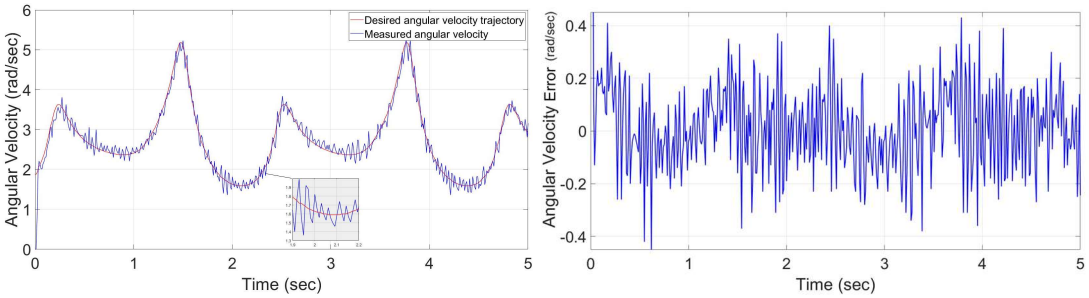

Fig. 16. a) Comparison of desired and measured crank speeds and b) crank speed error of Model-2 mechanism for $V_c^{des} = 0.1\ m/sec$

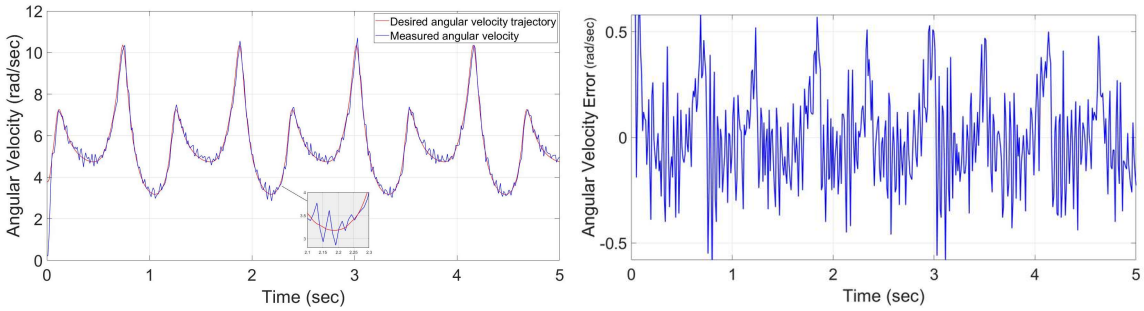

Fig. 17. a) Comparison of desired and measured crank speeds and b) crank speed error of Model-2 mechanism for $V_C^{des} = 0.2\ m/sec$

5.1. Comparison of numerical and experimental results

In this section, the desired coupler point velocities obtained from the numerical simulation and the experimental studies are compared. The results are given in Fig.s 18-21. It can be seen in all of the Fig.s, the coupler point velocities determined by the numerical simulation oscillate around the desired value of which and they continue to decrease during the time. A similar situation also exsists in the experimental cases but there are noise and sudden ups and downs. Approximate maximum deviations from desired velocity values for all cases are given in Table 3.

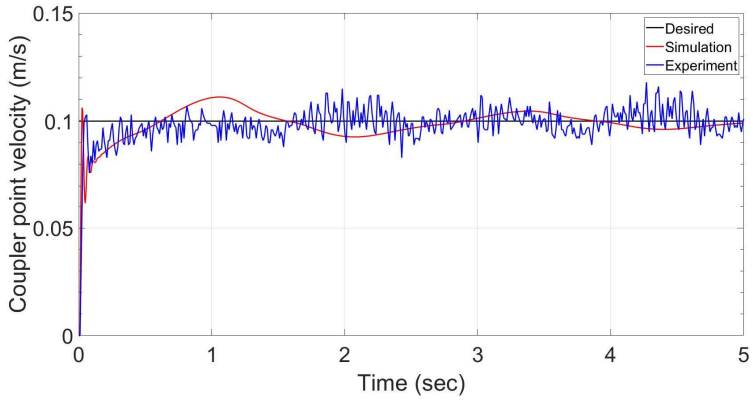

Fig. 18. Comparison of the couplar point velocities: desired, numerical simulation and experimental case for $V_C^{des} = 0.1\ m/s$ (Model 1)

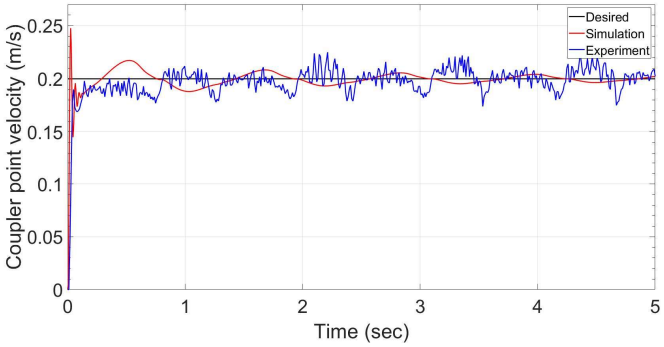

Fig. 19. Comparison of the couplar point velocities: desired, numerical simulation and experimental case for $V_C^{des} = 0.2\ m/s$ (Model 1)

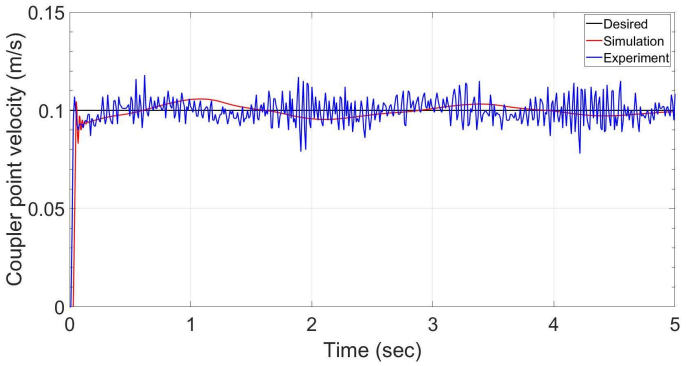

Fig. 20. Comparison of the couplar point velocities: desired, numerical simulation and experimental case for $V_C^{des} = 0.1\ m/s$ (Model 2)

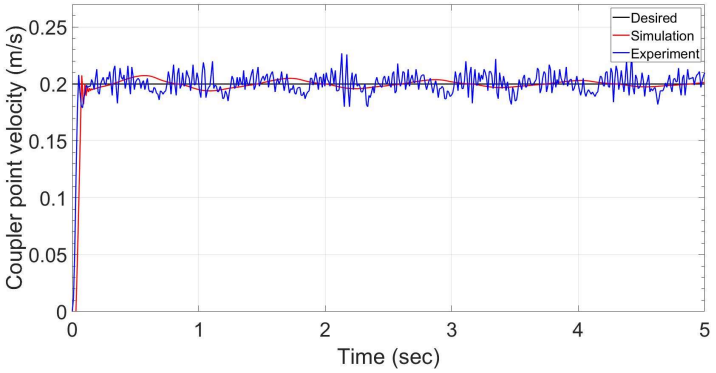

Fig. 21. Comparison of the couplar point velocities: desired, numerical simulation and experimental case for $V_C^{des} = 0.2\ m/s$ (Model 2)

Table 3. The maximum deviations for numerical and experimental case studies

Mechanism	Desired Velocity	Maximum Deviation (m/s)	
		Simulation	Experimental
Model 1	0.1	0.01	0.020
	0.2	0.01	0.025
Model 2	0.1	0.01	0.025
	0.2	0.01	0.025

In Table 3 and Figs. 18 through 21, it can be seen that the deviations in both the numerical and experimental case studies are acceptable. These minor deviations do not significantly impact the overall system performance or reliability. The deviations in the experimental case studies are bigger than that of the numerical simulations. However, the coupler point velocity approaches to the desired value as time progress in the numerical simulations while it goes up and down about reference value in the experimental case. This is an expected result. Because the sampling rate of the experimental system is lower than that of the numerical simulation due to frequency of the microprocessor used in the system. On the other hand, the mechanical issues such as loosness and manufacturing tolerances affect the experimental results. It is no doubt that the mechanical system works perfectly in the numerical simulation but it cannot fully represent the real mechanical structure. Nevertheless, the rise time is 0.07 sec and the settling time is 1.5 sec for all cases. As a result, it can be said that the desired velocity is achieved in both the numerical and experimental studies.

The numerical and experimental results are also compared for the desired velocities 0.1, 0.2, 0.3 and 0.4 m/sec in Fig. 22 for Model-1 and Model-2 mechanisms. It is seen that the deviations become larger as the desired velocity increases.

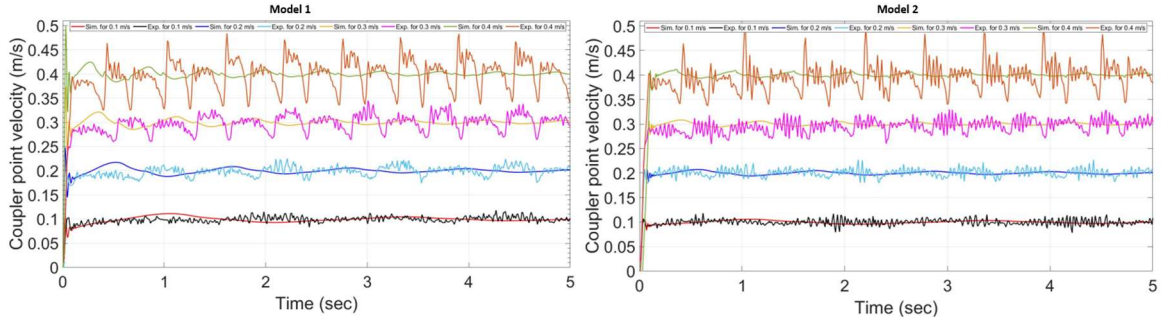

Fig. 22. Comparison of the couplar point velocity for different values: a) Model-1 b) Model-2

6. Conclusion and Discussion

The numerical simulations and the experimental case studies are made in order to show the efficiency of the method. Different constant couplar point velocity are considered in the case studies. However, the effect of the mass properties of the link 3 is investigated. It is shown that the constant coupler velocity could be achieved by the variable crank speed. The couplar point velocity approaches to the desired value as time progress in the numerical simulations. But there are sudden ups and downs about reference value in the experimental case. This is due to sampling rate of the microprocessor and the motor encoder, and some mechanical issues. As a result, MSM can provide analysis of the mechatronic systems without deriving the complex mathetmatical model as long as the parameters of the system are set accurately.

The experimental results demonstrate that for industrial applications requiring a stable speed, the system can maintain a speed of up to 0.2 m/s with oscillations around 0.025 m/s. This finding suggests that a low-cost system, designed to handle specified loads, could be effectively implemented for applications within this speed range. At target speeds of 0.3 m/s and 0.4 m/s, however, the system experiences increased fluctuations of about 0.04 m/s and 0.1 m/s along the trajectory, respectively. This knowledge allows for a well informed system selection, acknowledging that at higher speeds, speed stability may be compromised. Therefore, the system configuration can be chosen based on the allowable oscillation range, ensuring a balance between cost-effectiveness and performance requirements.

Conflict of Interest Statement

The authors declare that there is no conflict of interest.

References

[1] E. Söylemez, *Mechanisms,* MMO Middle East Technical University publication number 64, 1985.

[2] J. Tao and J.P Sadler, "Constant speed control of a motor driven mechanism system," *Mechanisms and Machine Theory,* vol. 30, no. 5, pp. 737-748, 1995. doi: 10.1016/0094-114X(94)00072-S

[3] Ö. Gündoğdu and K. Erentürk, "Fuzzy Control of a dc motor driven four-bar mechanism," *Mechatronic*, Cilt:15, s:423-438, 2005. doi: 10.1016/j.mechatronics.2004.10.004

[4] G. Şevkat ve S. Telli, "Elektrik Motoru İle Tahrik Edilen Dört Çubuk Mekanizmasının Kayan Kip Hız Kontrolu," *Uludağ Universitesi Mühendislik-Mimarlık Dergisi*, Cilt:13, No:2, s: 15-26, 2008. doi: 10.17482/uujfe.96125

[5] O. Çakar and A.K.Tanyildizi, "Application of moving sliding mode control for a DC motor driven four-bar mechanism," *Advances in Mechanical Engineering*, vol.10, no. 3, pp. 1–13, 2018. doi: 10.1177/1687814018762184

[6] M. Salah, A. Al-Jarrah, E. Tatlicioglu et al. "Robust Backstepping Control for a Four-Bar Linkage Mechanism Driven by a DC Motor," *J Intell Robot Syst,* vol. 94, pp. 327–338, 2019. doi: 10.1007/s10846-018-0811-y

[7] G. O Koca, Z. H Akpolat and M. Özdemir, "Type-2 fuzzy sliding mode control of a four-bar mechanism," *Int J Model Simul,* vol. 31, pp. 60–68, 2011. doi: 10.2316/Journal.205.2011.1.205-5335

[8] A. Al-Jarrah, M. Salah, K.S. Banihani, et al. "Applications of various control schemes on a four-bar linkage mechanism driven by a geared DC motor," *WSEAS Trans Syst Contr,* vol. 10, pp. 584–597, 2015. https://api.semanticscholar.org/CorpusID:11080447

[9] C.F. Chang, "Synthesis of adjustable four-bar mechanisms generating circular arcs with specified tangential velocities," *Mechanism and Machine Theory*, vol. 36, no. 3, pp. 387-395, 2001. doi: 10.1016/S0094-114X(00)00049-5

[10] H. S. Yan and R. C. Soong, "Kinematic and dynamic design of four-bar linkages by links counterweighing with variable input speed," Mechanism and Machine Theory, vol. 36, no. 9, pp. 1051-1071, 2001. doi: 10.1016/S0094-114X(01)00032-5

[11] R. Peón-Escalante, M. Flota-Bañuelos, L. J. Ricalde, C. Acosta, G. S. Perales, "On the coupler point velocity control of variable input speed servo-controlled four-bar mechanism," *Advances in Mechanical Engineering*, vol. 8, no. 11, pp. 1–9, 2016. doi: 10.1177/1687814016678356

[12] M. Flota-Bañuelos, R. Peón-Escalante, L. J. Ricalde, B. J. Cruz, R. Quintal-Palomo, J. Medina, "Vision-based control for trajectory tracking of four-bar linkage," *J Braz. Soc. Mech. Sci. Eng*, vol. 43, no. 324, pp. 1–11, May. 2021. doi: 10.1007/s40430-021-03043-z

[13] R. Peón-Escalante, M. Flota-Bañuelos, R. Quintal-Palomo, L.J. Ricalde, F. Peñuñuri, B. Cruz Jiménez and J. Avilés Viñas, "Neural Network Based Control of Four-Bar Mechanism with Variable Input Velocity," *Mathematics*, vol. 11, no.2148, pp. 1-17, 2023. doi: 10.3390/math11092148

[14] O. Denizhan and M. S. Chew, "Linkage mechanism optimization and sensitivity analysis of an automotive engine hood," *International Journal of Automotive Science and Technology*, vol. 2, no. 1, pp. 7-16, 2018. doi: 10.30939/ijastech..364438

[15] Matlab, 2021,(n.d.).https://www.mathworks.com/products/simmechanics.html. [Accessed: Feb. 1, 2025].

[16] H. Hülako and O. Yakut, "Control of Three-Axis Manipulator Placed on Heavy-Duty Pentapod Robot," *Simul. Model Pract. Theory*, vol. 108, no. May 2020, 2021. doi: 10.1016/j.simpat.2020.102264